J MATER SCI 41 (2006) 1683–1690

Shock and release of polycarbonate under one-dimensional strain

J. C. F. MILLETT*
Defence Academy of the United Kingdom, Cranfield University, Shrivenham, Swindon, SN6 8LA, U K
E-mail: j.c.f.millett@cranfield.ac.uk

N. K. BOURNE
School of Aerospace, Mechanical and Civil Engineering, University of Manchester, Sackville Street, Manchester, M60 1QD, U K

Published online: 17 February 2006

The behaviour of the thermoplastic polycarbonate has been investigated using manganin stress gauges in both longitudinal and lateral orientations. These have been used to determine the shock stress, shock velocity, particle velocity, release velocity and shear strength. The relationship between shock velocity and particle velocity has been shown to be linear, with the value of c_0 (the zero particle velocity intercept of shock velocity) equating to the measured bulk sound speed. This behaviour is more commonly observed in metals. Shear strength has been observed to increase behind the shock front, a feature observed in other polymers such as PMMA or PEEK. It also increases with stress amplitude, although the projected intercept with the calculated elastic response indicates that the Hugoniot elastic limit (HEL) is lower than in other polymers, for example PMMA (ca. 0.75 GPa) or PEEK (ca. 1.0 GPa). This further suggests that the yield strength of polycarbonate does not obey a Mohr-Coloumb criterion, and hence is not as strongly pressure dependent as other polymers.

1. Introduction

The response of materials to high loading rate situations is an area of great importance and increasing interest. The traditional driving force for such research has lain with the military in armour, armour defeat mechanisms and response to explosive loading, but more recently, other fields have come to appreciate such measurements. This includes the aerospace industry (bird strike, foreign object damage and blade containment), the automotive industry (crashworthiness testing), satellite protection from orbital debris, and high speed forming and machining operations. Unfortunately, a high loading rate event such as an impact tends to be complex. For example, the "target" (such as a blade in an aero engine) is likely to have a complex geometry, and the projectile itself can strike at an arbitrary angle and velocity. Therefore, the resulting stress and strain state imposed by the impact can contain all conditions (compression, tension and shear), making the results near impossible to analyse in any meaningful way. By simplifying the loading geometry, material response becomes more tractable, and thus mechanical properties and microstructural behaviour can be extracted for inclusion in computer models that are used to predict more realistic events. At quasi-static strain-rates, such tests include tension and compression loading in one-dimensional stress or plane-strain fracture toughness. At higher strain-rates (ca. 10^3 s^{-1}), the split Hopkinson compression bar can also place materials into one-dimensional stress, but at higher strain-rates still, inertia effects render such loading impossible. Such strain-rates can be imposed by a number of techniques, including launching a shock wave into a target, either explosively, or by the technique of plate impact. In this latter, an accurately machined flyer plate (flat and parallel to better than ± 5 μm) of known response is impacted onto an equally flat and parallel target or specimen plate, instrumented such that useful information may be measured. As a rule, impact velocities are a minimum of ca. 100 ms^{-1}. The impact of the flyer plate generates a planar shock wave, behind which, conditions of one-dimensional strain apply. In this situation, all strain

*Author to whom all correspondence should be addressed.
0022-2461
DOI: 10.1007/s10853-006-3951-6

is accommodated along the impact axis (ε_x), whilst the orthogonal components (y and z) are zero due to inertial confinement. Correspondingly, while there is an impact or longitudinal stress (σ_x), the orthogonal components of stress, to maintain confinement, must, by definition be non-zero, thus,

$$\varepsilon_x \neq \varepsilon_y = \varepsilon_z = 0 \quad \text{and} \quad \sigma_x \neq \sigma_y = \sigma_z \neq 0 \qquad (1)$$

A full description of this one-dimensional shock loading technique is beyond the scope of this paper. However, the reader is directed to the review article of Davison and Graham [1] for a more complete description of the shock loading of solids.

The response of polymeric materials to shock loading has only recently begun to attract significant attention. A major source of interest has been from the energetic materials community, where polymers such as polychlorotrifluroethylene (Kel-F) [2], estane (a polyurethane rubber) [3] and hydroxy terminated polybutadiene (HTPB) [4] are used as binder systems in plastic bonded explosives (PBXs). Epoxy based fibre composites have also attracted interest as light-weight armours [5], and thus the shock response of various epoxies have been studied [6, 7]. Despite this, polymers have not had the detailed attention that other materials such as metals have, the main exception being polymethymethacrylate (PMMA) [8] as it is used as a window material in interferometric velocity measurements during shock experiments, requiring a detailed understanding of its shock response.

The most extensive work to date on polymers has been performed by Carter and Marsh [9]. Their results showed that many polymers, especially those with open structures such as benzene rings experienced a structural change at a shock pressure of ca. 20 GPa. It was suggested that this was caused by the breakdown of the bonds in the benzene rings, and their reformation as tetragonal bonds between the polymer chains, in a manner analogous to the graphite to diamond phase transformation. Kargin *et al.* [10] recovered shocked polymers for analysis. Their results in simple thermoplastics showed that significant structural rearrangement occurred in the form of spherulite size changes. Here size increased with shock pressure, suggesting that the mobility of structural blocks increase with pressure. However, no evidence of melting was observed, nor changes in chemistry, even up to pressures of 40 GPa. Our own investigation into the shock response of HTPB [4] showed no changes in glass transition temperature (T_g), decomposition temperature or molecular weight occurred, although these were to more modest pressures of ca. 1.5 GPa.

There isn't a great deal of published data concerning the behaviour of polycarbonate during shock loading. Curran *et al.* [11] investigated the dynamic tensile (spall) behaviour, due to the interactions of release waves from the rear of the flyer and target plates creating a plane of net tension in the body of the target. Their results suggested that damage is nucleated at pre-existing defects, with cracks initially growing slowly but accelerating towards the Rayleigh wave speed. As the cracks coalesced, it was observed that they had a dished shape, as opposed to the more expected penny shape. This was attributed to the stress field at the crack tips changing the direction of crack growth towards each other. de Resseguier and Deleignies [12] also observed dished shaped cracks due to laser induced spallation of polycarbonate, again due to interaction between cracks and the associated stress fields. They also used electromagnetic particle velocity gauges to determine the equation of state, showing similar results to those of Carter and Marsh [9] who included polycarbonate in their compendium of the shock response of polymers. Finally, they noted that the shape of the particle velocity traces was very sharp, suggesting that viscous effects (i.e. a rounding of the pulse as it approaches its maximum amplitude, as observed in PMMA by Barker and Hollenbach [8]) were not as appreciable as in some other polymers, although it should be pointed out that the amplitude of this particular set of experiments was in the range 9 to 70 GPa. In this paper, we investigate the equation of state of polycarbonate at low pressures, and compare it to existing data. We also examine the release response from the shocked state, and finally, measure the strength behind the shock front, and its variation with stress amplitude.

2. Experimental

All shots were performed using a 5 m long, 50 mm bore single stage gas gun [13]. Two sets of experiment were performed. In the first, the equation of state was determined in terms of shock stress, shock velocity and particle velocity. Target assemblies were made by fixing a manganin stress gauge (MicroMeasurements type LM-SS-025CH-048) between 5 or 6 mm plates of polycarbonate with a low viscosity epoxy adhesive. A second gauge (the 0 mm position) was supported on the front with a 1 mm plate of either dural (aluminium alloy 6082-T6) or copper, which was matched to the material of the flyer plate. In this way, both shock stress (from the amplitude of the signal) and shock velocity through the known spacings of the gauges in terms of position within the target assembly (Δw) and time (Δt_{shock}) could be determined ($U_s = \Delta w/\Delta t_{\text{shock}}$). Gauge calibrations were according to Rosenberg *et al.* [14]. Impact stresses were generated by 5 mm dural or copper flyer plates impacted in the velocity range 200 to 1087 ms^{-1}. Impact velocities were measured by the shorting of sequentially mounted pairs of pins to an accuracy of 0.5%. Particle velocities, that is the velocity of material flow behind the shock front, (u_p) were determined from the known response of the flyer plate materials [15], the measured impact velocity and the measured longitudinal stresses from the gauges using impedance matching techniques. The second set of experiments measured the lateral component of stress (σ_y), and from that, the shear strength behind the shock front (2τ)

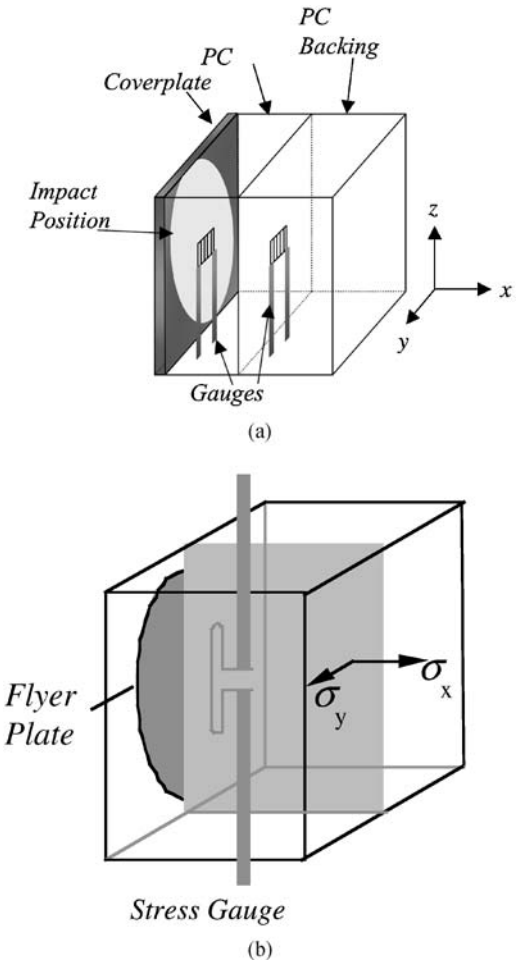

Figure 1 Schematic of target assemblies including gauge placements (a) Longitudinal stress measurements: (b) Lateral stress measurements.

through the well-known relation,

$$2\tau = \sigma_x - \sigma_y. \tag{2}$$

In this case, manganin gauges of a different type (MicroMeasurements J2M-SS-580SF-025) were introduced into sectioned 10 mm plates of PC, 4 mm from the impact face. The targets were re-assembled using a low viscosity adhesive, and held in a special jig for a minimum of 12 h. Afterwards, the impact face was lapped flat to no greater than 5 optical fringes from a monochromatic light source, across 50 mm. Lateral stresses were determined from the work of Rosenberg and Partom [16], using a modified analysis that does not require knowledge of the longitudinal stress [17]. Finally, we also had to take into account that the particular gauge used has a different response to the more familiar grid gauges at low stresses [18]. Specimen alignment was controlled by a machinable end piece to the gun barrel. Specimen configurations and gauge placements are presented in Fig. 1.

The acoustic properties were measured using quartz transducers in longitudinal and shear orientation at 5 MHz, using a Panametrics PR5077 pulse receiver.

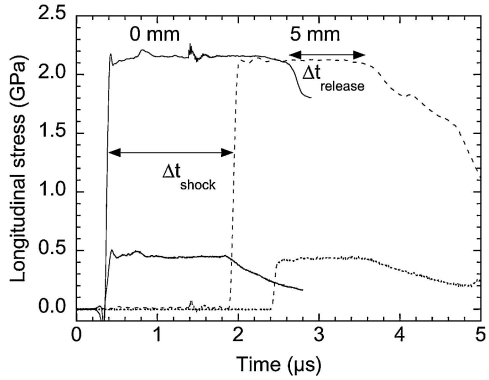

Figure 2 Longitudinal stress gauge traces in polycarbonate. The impact conditions are −5 mm dural flyer at 200 ms^{-1} (lower amplitude traces) and 5 mm copper flyer at 605 ms^{-1}.

3. Materials data

Polycarbonate is a glassy polymer that has approximately 0.7% of total polymer market share [19]. It finds application in wind-screens and helmet visors. It has also been used as a laminate in armoured glasses, and thus knowledge of its shock response is of interest. The elastic properties are detailed in Table I. We also include the same properties collected by Carter and Marsh [9] for comparison.

4. Results

In Fig. 2, we present traces from longitudinal stress measurements in polycarbonate.

The traces labelled 0 mm can only be used to determine the stress amplitude, as the shock measured at this point will only have travelled through 1 mm of either dural or copper. The traces labelled 5 mm will however, have measured the stress after it has travelled through 5 mm of polycarbonate, and thus their shape will be modified by the material properties. Note that under both impact conditions (and indeed all others) the stress levels at both positions are the same, showing that no attenuation has occurred. The shape of the pulses at this position in both cases is square, showing no evidence of rounding as the stress reaches its final amplitude. Finally, in the high amplitude traces, arrows labelled Δt_{shock} and $\Delta t_{\text{release}}$ have been used to demonstrate the temporal spacings used to determine the shock velocity and release velocities respectively.

In Fig. 3, we have used the shock velocities, measured using the temporal spacings discussed above and the method in the experimental section to show its variation with particle velocity. We have also included the data of Carter and Marsh [9] and Mori and Nagayama [20].

Straight lines have been fitted to each set of data, based on the assumption that the shock velocity—particle velocity relationship (in common with many other materials) is based on the form,

$$U_s = c_0 + Su_p, \tag{3}$$

TABLE I Material properties of polycarbonate.

	c_L – mm μs^{-1}	c_s – mm μs^{-1}	c_B – mm μs^{-1}	ρ_0 – kg m^{-3}	ν
This work	2.13 ± 0.03	0.88 ± 0.03	1.87 ± 0.03	1190 ± 20	0.40
Ref. [9]	2.19	0.89	1.93	1200	0.40

where c_0 and S are the shock parameters. Although these are purely empirically determined values, c_0 has, in metals at least, been correlated with the experimentally determined bulk sound speed, c_B, whilst S has been shown to relate to the first derivative of bulk modulus with pressure [1]. It can be seen that the magnitude of all three sets of data agree closely, but when straight line fits according to Equation 3 are used, differences become apparent. In our results, this has yielded the relation, $U_s = 1.87 + 2.41u_p$. In Carter and Marsh [9], $U_s = 2.33 + 1.57u_p$ is quoted, whilst the corresponding data for Mori and Nagayama [20] gives $U_s = 2.18 + 1.82u_p$, and for de Resseguier and Deleignies [12], $U_s = 2.20 + 1.53u_p$. Note that Carter and Marsh obtained their data over a much wider particle velocity range (0.4 to 2.6 mm μs^{-1}). In the case of Mori and Nagayama, only their point at a particle velocity of ca. 0.15 mm μs^{-1} was measured, the higher points were obtained from the compendium published by Marsh [15], which in fact uses the same data as Carter and Marsh [9]. In our own data, it is interesting to observe that our value of c_0 of 1.87 mm μs^{-1} agrees precisely with the experimentally determined value of bulk sound speed shown in Table I ($c_B = 1.87 \pm 0.03$ mm μs^{-1}).

In the following figure, we show the shock Hugoniot of polycarbonate, in terms of the shock stress (determined from the amplitude of the signals presented in Fig. 2) and the particle velocity (from impedance matching). Also included is the data of Carter and Marsh [9] for comparison. The solid curve is the calculated hydrodynamic pressure (P_{HD}), determined via,

$$P_{HD} = \rho_0 U_s u_p, \tag{4}$$

where ρ_0 is the ambient density, and U_s is our own experimentally measured shock velocity data presented in Fig. 3. It can be seen that our own stress data agrees with that of Carter and Marsh at lower stresses, but becomes significantly greater at higher particle velocities, whilst our calculated hydrodynamic response is in close agreement with the previously published data. This is a feature that we have observed in a number of other polymers [21] and will be discussed later in the text.

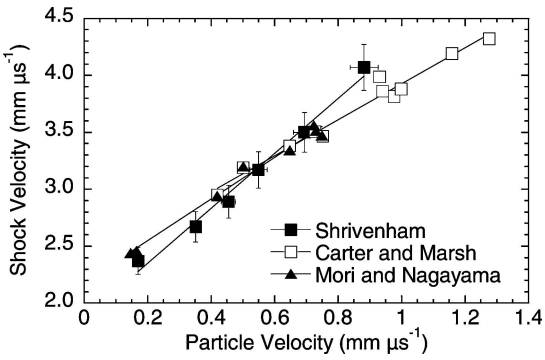

Figure 3 Shock velocity versus particle velocity for polycarbonate. We have also included the previous data from Carter and Marsh [9] and Mori and Nagayama [20].

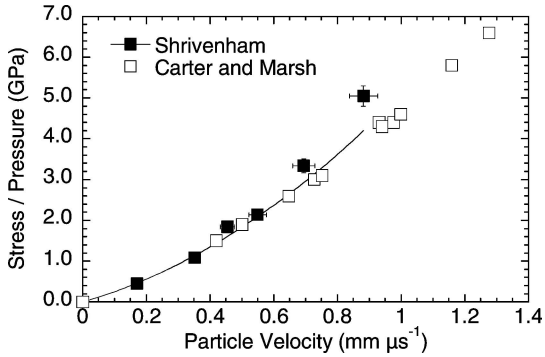

Figure 4 The shock Hugoniot of polycarbonate, including previous results from Carter and Marsh [9] and Mori and Nagayama [20]. The curve is the calculated hydrodynamic pressure, using equation [4] and our experimentally determined shock velocities.

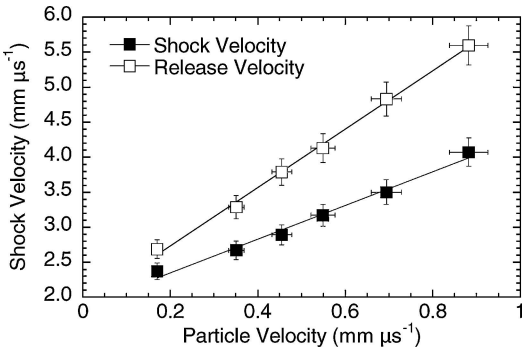

Figure 5 Comparison of experimentally measured shock and release velocities as a function of particle velocity. Release velocities were calculated using equation [5].

In Fig. 5, we present the release velocities in polycarbonate as a function of particle velocity. We have also included our own shock velocity data from Fig. 3 as a comparison.

Release velocities (U_R) were calculated from,

$$U_R = \frac{\Delta w}{\Delta t_{release}} \left(1 - \frac{u_p}{U_S}\right), \tag{5}$$

which takes into account that the release waves will be initially moving into shock compressed material. We have fitted a straight line to this data of the form, $U_R = A + Bu_p$,

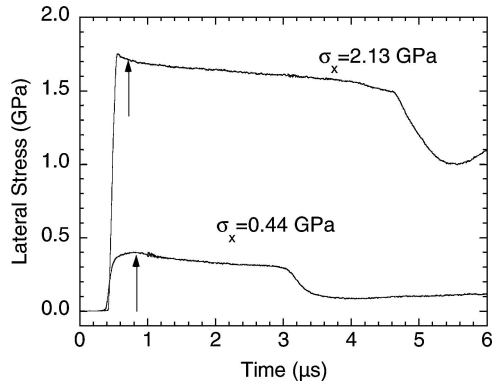

Figure 6 Representative lateral stress traces in polycarbonate. Impact conditions are −10 mm dural flyer at 200 ms^{-1} ($\sigma_x = 0.44$ GPa), and 10 mm copper flyer at 579 ms^{-1} ($\sigma_x = 2.13$ GPa). The gauges are 4 mm from the impact face.

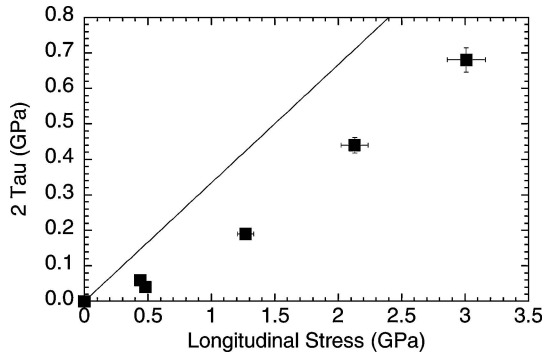

Figure 7 Shear strength versus longitudinal stress. The straight line is the calculated elastic response according to equation [6], using the experimentally determined value of ν.

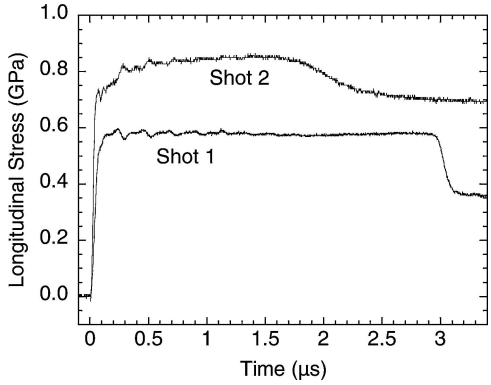

Figure 8 Embedded stress gauge traces in PMMA Shot 1. 10 mm dural flyer at 207 ms^{-1}. Gauge 9 mm from impact. Shot 2−4.96 mm copper flyer at 258 ms^{-1}. Gauge 13 mm from impact.

yielding $A = 1.90$ mm μs^{-1} and $B = 4.16$. We would also point out that the value of A, at 1.90 mm μs^{-1}, is close to the value of c_0 (from the shock velocity) of 1.87 mm μs^{-1}, and within the error bound of the bulk sound speed, 1.87 $\pm$ 0.03 mm μs^{-1}.

In Fig. 6, representative traces from lateral stress gauges are shown. There are a couple of features present in these traces that require attention. Firstly, the low stress trace has a significantly lower duration than the high stress trace. This may be explained by the fact that at 0.44 GPa, a dural flyer was used, with a longitudinal wave speed of ca. 6.4 mm μs^{-1}, compared to 2.13 GPa, where a copper flyer, with a wave speed of ca. 4.8 mm μs^{-1} was used. In this flyer/specimen geometry, release waves from the rear of the flyer will reach the gauge location before releases from the rear of the target. Thus the pulse durations are explained. More significantly, observe that in both traces, lateral stress decreases significantly behind the shock front. This is a feature that we have observed in a number of other polymers such as PMMA [22], epoxy resins [7] and PEEK [23]. Gupta and Gupta [24] also observed this response in PMMA during lateral stress measurements in PMMA, although no comment was made at the time. From Equation 2, this suggests that the shear strength in polycarbonate *increases* behind the shock front.

Finally, in Fig. 7, we present the variation of shear strength with longitudinal stress. The shear strengths were determined from Equation 2, using the lateral stress immediately behind the shock front, as indicated by the arrows in Fig. 6.

The straight line is the calculated elastic response, according to,

$$2\tau = \frac{1-2\nu}{1-\nu}\sigma_x, \tag{6}$$

using the calculated Poisson's ratio shown in Table I.

It can be seen that the at all longitudinal stress levels, the shear strength lies significantly below the HEL of polycarbonate. This implies that the material has already yielded, even at the lowest of the stresses in this investigation.

5. Discussion

A series of experiments have been performed to probe the shock response of polycarbonate. In Fig. 2, we showed that the stress pulse as it passed through the polycarbonate was largely square in nature, even at higher stresses. We have observed such a response in other polymers such as PEEK [23] and HTPB [4], which we have equated with a linear $U_s - u_p$ relationship. In contrast, PMMA [8], where a pronounced rounding at the top of the shock pulse above the HEL was seen and attributed to a significant non-linearity in $U_s - u_p$ at lower particle velocities, this behaviour was not observed. We illustrate this point in Fig. 8, where stress measurements in PMMA above and below the HEL show very different behaviours. This figure clearly shows that PMMA below the HEL of ca. 0.75 GPa possesses a square natured pulse, and a rounded one above. The non-linear nature of the $U_s - u_p$ relationship in PMMA is readily apparent in comparison with that of polycarbonate, as shown in Fig. 9.

In PMMA, this was explained in terms of the high strain-rate sensitivity in regard to its inelastic response.

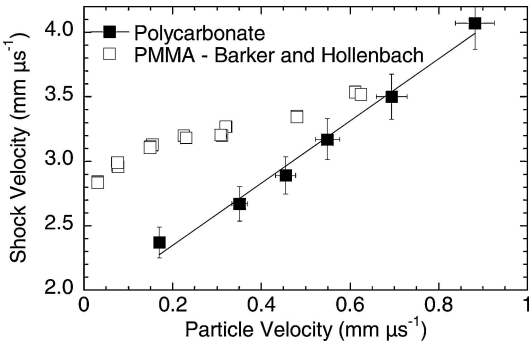

Figure 9 Comparison of shock velocity and particle velocity between polycarbonate and PMMA [8].

Certainly, at quasi-static strain rates, Goble and Wolff [25] have shown that the strain-rate sensitivity, $m = \delta \ln\sigma / \delta \ln\dot{\varepsilon}$ in PMMA is over twice that of polycarbonate (0.0418 and 0.0191 respectively). Therefore, the lower strain-rate sensitivity in polycarbonate may account for the more linear response in $U_s - u_p$. We also note with interest that the particle velocity traces of de Resseguier and Deleignies [12] were also very sharp with no evidence of rounding as the maximum amplitude was approached.

From Fig. 3, we also observe that although our own $U_s - u_p$ data is linear, as is that of Carter and Marsh [9] and Mori and Nagayama [20], there are differences in the values of c_0 and S. Firstly, we point out that the higher particle velocity data of the latter authors was obtained from the shock compendium of Marsh [15], which ultimately means it is the same data as that of the former. Therefore, it perhaps not surprising that there is closer agreement between the two. Our own data has a higher value of S, but is taken over a lower particle velocity range than Carter and Marsh, although there is some overlap between the two at the upper end of our particle velocity range. Given that both sets of data are linear in nature, supported by the observations made above, an explanation is required. One possible solution lies in the elastic data presented in Table I. Here, it can be seen that the bulk sound speed of our material is rather lower than that of Carter and Marsh [9]. Given that this is a function of the bulk modulus, it indicates that the resistance to elastic deformation will increase with increasing bulk modulus. As it has been suggested by Davison and Graham [1] that S is related to the first pressure derivative of bulk modulus, it is likely that a high bulk modulus material will also have a high resistance to change of that parameter, thus reducing S. As these two sets of data have been collected several decades apart, this may reflect that small differences in chemistry can have a significant effect on the shock response. In studying two HTPB compositions [4], we showed that a commercial composition, with added plasticizers had a lower density, similar sound speed and higher S than a pure HTPB without such additives.

The shock Hugoniot of polycarbonate presented in Fig. 4 shows a small deviation between our measured stress values and those of Carter and Marsh [9]. However, the agreement between Carter and Marsh and our calculated hydrodynamic pressure, over the particle velocity range we measured is good. The reason lies in the way the two sets of data were measured. In our own, we have measured the longitudinal stress, which is expressed in solid mechanics as a hydrostatic pressure (P) plus a shear strength components, thus,

$$\sigma_x = P + \frac{4}{3}\tau. \tag{7}$$

In contrast, Carter and Marsh [9] monitored the rear surface velocity of their targets (in effect the particle velocity) with streak cameras. Therefore, with knowledge of the shock velocity they used Equation 4 to calculate the hydrodynamic pressure. This is reflected in the close agreement between their pressure values and our calculated hydrodynamic response. However, the differences between the hydrodynamic pressure and the measured stress has implications for the materials strength behind the shock front. Although the hydrodynamic and hydrostatic pressures will not be precisely the same, they are sufficiently close that from Equation 7, the differences between measured stress and calculated pressure suggest (qualitatively at least) that the shear strength has a positive dependence on longitudinal stress. This pattern has been observed in a number of other polymers, including polyethylene, polypropylene, polystyrene [21] and PEEK [23]. Certainly in the case of the latter, this variation of shear strength with longitudinal stress was confirmed independently via lateral stress measurements using Equation 2. Further, in the elastomer, polychloroprene [26], close agreement between longitudinal stress and calculated hydrodynamic pressure suggested that shear strength was constant with increasing longitudinal stress, again demonstrated independently with lateral stress measurements.

Before moving on to discuss the lateral stress measurements, we would like to make a final comment about the shock velocity and release velocity results presented in Fig. 5. Both data sets are clearly linear over the experimental range of this investigation, with the release speeds greater than the shock velocity. Linear regression fits yield relationships in terms of particle velocity of $U_s = 1.87 + 2.41u_p$ and $U_R = 1.90 + 4.16u_p$ for shock and release velocities respectively. Observe that the zero particle velocity intercepts (1.87 mm μs^{-1} for the shock velocity and 1.90 mm μs^{-1} for the release velocity) are near identical. This implies that the material returns to its ambient condition after release, without other factors such as phase transformations occurring. Phase transformations have been observed in polymers, the notable example being polytetrafluroethylene (PTFE). Champion [27] observed a change in slope of $U_s - u_p$ corresponding to a shock pressure of ca. 0.5 GPa, similar to static pressure measurements of 0.54 GPa. A final interest lies in a comparison between the value of c_0 determined from the shock velocity measurements (1.87 mm μs^{-1}) and the ambient pressure bulk sound speed, c_B, measured using quartz

transducers (1.87 ± 0.03 mm μs^{-1}). As can be seen, these two values are identical at the frequency of the transducer. This behaviour is commonly seen in metals such as copper or nickel [15], but is generally not seen in polymers. In their assessment of twenty-one polymers, Carter and Marsh [15] showed that in all cases, c_0 was greater than c_B. Indeed, in sixteen of those polymers, including polycarbonate, they showed that c_0 was greater than the longitudinal sound speed, c_L. Mori and Nagayama [20] have also observed this behaviour in polypropylene, nylon 6, polyvinylchloride and PTFE, although it was not commented on, and we ourselves have observed such behaviour in a range of polymers including an epoxy resin [7], PEEK [23], HTPB [4], polypropylene [21], polychloroprene [28] and the fluorinated trimer, Viton-B [29]. Even in materials where we observed that c_0 was lower than c_L such as polyethylene and polystyrene [21], it was still significantly above the bulk sound speed, in common with the observations of Carter and Marsh [9]. Therefore, it would appear that the polycarbonate studied in this paper has a response more akin to metallic materials than other polymers, although at present, the reasons for this are still unclear.

In Fig. 6, the lateral gauge traces show a clear decrease in stress behind the shock front. Using Equation 2, and assuming that longitudinal stress remains constant (which from Fig. 2 it clearly does), thus indicates that the shear strength increases behind the shock font. Such a response has been observed in metals, for example titanium aluminides [30] where it has been equated with dislocation and/or twin generation behind the shock front. Such a response is not possible in a polymer, hence another explanation is sought. This behaviour has been observed in other polymers such as PMMA [22], epoxy [7] and PEEK [23]. In those works, it was suggested that this was a manifestation of the viscoplastic response of such materials.

Finally, from Fig. 7, it can be seen that the shear strength of polycarbonate increases with increasing longitudinal stress. However, comparison with the calculated elastic response shows that the measured strength lies significantly below. As with the observations made concerning the relationship of shock velocity with particle velocity, this appears to be a deviation from behaviour observed in other polymers. For example in PMMA [22], epoxy [7] and PEEK [23], agreement between the two at lower stresses allowed an estimation of the HEL to be made, which in the case of PMMA at least could be verified against the results of others [8]. In PMMA, Rosenberg and Partom [31] also accounted for the large increase in shear strength, from ca. 50 MPa at quasi-static strain-rates to 750 MPa during shock loading, by assuming that it obeys a Mohr-Colulomb yield criterion. In contrast, in polycarbonate (Fig. 7), results would suggest that by extrapolating the shear strength back towards the calculated elastic response, the HEL is very low. Rabinowitz *et al*. [32] pointed out that other factors such as degree of crystallinity can effect the sensitivity of yield strength with pressure. However, it is clear that shear strength itself has a strong positive dependence on longitudinal stress, and hence pressure. The observed trends of our shear strength measurements also lend credence to the suggestion made in Fig. 4, that, due to the increasing differences between the measured stress and calculated hydrodynamic pressure, the strength of the material increased at higher stresses.

6. Conclusions

The shock response of polycarbonate has been monitored using manganin stress gauges. Our results show that shock velocity has a linear relationship with particle velocity, in common with many other materials. Our data is close to other values of these constants for the material presented in other works. We believe that this is due to differences in bulk modulus, which reflects in the higher values of c_0 and S suggesting that the material in this investigation having a slightly higher compressibility. The value of c_0 has been shown to have the same value of the measured bulk sound speed. This is a behaviour more commonly seen in metals. In polymers, c_0 is usually greater than the bulk sound speed, hence it seems that the shock response of polycarbonate is anomolous. Shear strength behind the shock front has been shown to increase with increasing stress amplitude. However, extrapolating back towards the calculated response, reveals that the HEL is very low in this material. This is in contrast to other polymers we have investigated, including PMMA, an epoxy resin and PEEK, where the HEL was shown to be much higher, of the order of hundreds of MPa. In those materials, it was suggested that they obeyed a Mohr-Coloumb yield criterion. The results presented here suggest that polycarbonate does not.

Acknowledgments

The authors would like to thank Matt Eatwell, Ivan Knapp and Gary Cooper for performing the shock loading experiments in this investigsation.

References

1. L. DAVISON and R. A. GRAHAM, *Phy. Rept.* **55** (1979) 255.
2. M. U. ANDERSON, in "Shock Compression of Condensed Matter – 1991," edited by S. C. Schmidt, R. D. Dick, J. W. Forbes and D. G. Tasker (North-Holland, Amsterdam, 1992), p. 875.
3. J. N. JOHNSON, J. J. DICK and R. S. HIXSON, *J. Appl. Phys.* **84** (1998) 2520.
4. J. C. F. MILLETT, N. K. BOURNE and J. AKHAVAN, *ibid.* **95** (2004) 4722.
5. W. RIEDEL, H. NAHME and K. THOMA, in "Shock Compression of Condensed Matter – 2003," edited by M. D. Furnish, Y. M. Gupta and J. W. Forbes (AIP Press, Melville, NY, 2004), p. 701.
6. D. E. MUNSON and R. P. MAY, *J. Appl. Phys.* **43** (1972) 962.
7. J. C. F. MILLETT, N. K. BOURNE and N. R. BARNES, *ibid.* **92** (2002) 6590.
8. L. M. BARKER AND R. E. HOLLENBACH, *ibid.* **41** (1970) 4208.

9. W. J. CARTER and S. P. MARSH, "Hugoniot Equation of State of Polymers" LA-12006-MS, Los Alamos National Laboratory, (1995).
10. V. A. KARGIN, G. P. ANDRIANOVA, I. Y. TSAREVSKAYA, V. I. GOLDANSKII and P. A. YAMPOLSKII, *J. Poly. Sci. A-2* **9** (1971) 1061.
11. D. R. CURRAN, D. A. SHOCKEY and L. SEAMAN, *J. Appl. Phys.* **44** (1973) 4025.
12. T. DE RESSEGUIER and M. DELEIGNIES, *Shock Waves.* **7** (1997) 319.
13. N. K. BOURNE, *Meas. Sci. Technol.* **14** (2003) 273.
14. Z. ROSENBERG, D. YAZIV and Y. PARTOM, *J. Appl. Phys.* **51** (1980) 3702.
15. S. P. MARSH, LASL Shock Hugoniot Data, University of California Press, Los Angeles, 1980.
16. Z. ROSENBERG and Y. PARTOM, *J. Appl. Phys.* **58** (1985) 3072.
17. J. C. F. MILLETT, N. K. BOURNE and Z. ROSENBERG, *J. Phys. D. Appl. Phy.* **29** (1996) 2466.
18. Z. ROSENBERG, N. K. BOURNE and J. C. F. MILLETT, *J. Appl. Phys.* (2005) Submitted.
19. N. J. MILLS, Plastics: Microstructure and Engineering Applications, Second (Arnold, London, 1993).
20. Y. MORI and K. NAGAYAMA, *SPIE* **3516** (1999) 241.
21. J. C. F. MILLETT and N. K. BOURNE, *J. Phys. D. App. Phy.* **37** (2004) 2901.
22. J. C. F. MILLETT and N. K. BOURNE, *J. Appl. Phys.* **88** (2000) 7037.
23. J. C. F. MILLETT, N. K. BOURNE and G. T. GRAY III *J. Phys. D. App. Phy.* **37** (2004) 942.
24. S. C. GUPTA and Y. M. GUPTA, *J. Appl. Phys.* **57** (1985) 2464.
25. D. L. GOBLE and E. G. WOLFF, *J. Mater. Sci.* **28** (1993) 5989.
26. N. K. BOURNE and J. C. F. MILLETT, *Proc. R. Soc. Lond. A* **459** (2003) 567.
27. A. R. CHAMPION, *J. Appl. Phys.* **42** (1971) 5546.
28. J. C. F. MILLETT and N. K. BOURNE, *ibid.* **89** (2001) 2576.
29. J. C. F. MILLETT, N. K. BOURNE and G. T. GRAY III, *ibid.* **96** (2004) 5500.
30. J. C. F. MILLETT, N. K. BOURNE, G. T. GRAY III and I. P. JONES, *Acta Mater.* **50** (2002) 4801.
31. Z. ROSENBERG and Y. PARTOM, *J. Appl. Phys.* **76** (1994) 1935.
32. S. RABINOWITZ, I. M. WARD and J. S. C. PARRY, *J. Mater. Sci.* **5** (1970) 29.

Received 20 April
and accepted 8 June 2005